Advanced Materials Research Vol. 364 (2012) pp 243-247
Online available since 2011/Oct/24 at www.scientific.net

doi:10.4028/www.scientific.net/AMR.364.243

Large-Area Synthesis and Microstructural Investigations of Silicon Nanowires and Te/Bi_2Te_3-Si Core-Shell Structures

NG Inn Khuan[1,a], KOK Kuan Ying[1,b], Siti Salwa Zainal Abidin[1,c], Nur Ubaidah Saidin[1,d] and Choo Thye Foo[1,e]

[1]Malaysian Nuclear Agency, Bangi, 43000 Kajang, Selangor D. E., MALAYSIA.

[a]ikn1000@nuclearmalaysia.gov.my, [b]kyk1000@nuclearmalaysia.gov.my, [c]ctsalwa79@yahoo.com, [d]ubaidah@nuclearmalaysia.gov.my, [e]ctfoo@nuclearmalaysia.gov.my

Keywords: Silicon nanowires, core-shell structures, self-selective electroless etching, solid-liquid-solid.

Abstract. Large-area randomly-oriented silicon nanowires (SiNWs) were synthesized using Au-coated p-type Si(100) substrates via the solid-liquid-solid (SLS) process under different growth conditions. Microstructural studies on the NWs produced showed that straight crystalline nanowires of large aspect ratios were generally obtained at a growth temperature of 1000°C along with some worm-like amorphous structures. Large-area vertically aligned silicon nanowire (SiNW) arrays on p-type (001) Si substrates were also synthesized in an aqueous solution containing $AgNO_3$ and HF by self-selective electroless etching. Diameters of the SiNWs produced from both methods varied from 50 nm to 350 nm and their lengths generally extended from several to approximately a few tens of μm depending on the growth conditions used. Te-Si and Bi_2Te_3-Si core-shell structures were subsequently obtained via galvanic displacement of SiNWs in acidic HF electrolytes containing $HTeO_2^+$ and $Bi^{3+}/HTeO_2^+$ ions. The reactions were basically a nano-electrochemical process due to the difference in redox potentials between the materials. The modified SiNWs of core-shell structures had roughened surface morphologies and, therefore, higher surface-to-bulk ratios compared to unmodified SiNWs. They should have potential applications in sensors, photovoltaic and thermoelectric nanodevices. Microstructural studies on the SiNWs and core-shell structures produced are presented using various microscopy, diffraction and probe-based techniques for characterization.

Introduction

In recent years, much effort has been devoted to growing SiNWs with controlled morphology, chemistry, microstructures, localization and device structures [e.g.1]. Among the different growth methods, Chemical vapor deposition (CVD) based on the vapor-liquid-solid (VLS) growth mechanism [2] has been the most established and widely used method for growing crystalline SiNWs as it provides good control over composition, size, crystallographic direction and location. SiNWs have also been grown via the solid-liquid-solid (SLS) route under high temperature using Au-coated silicon substrate as catalyst [3]. These techniques normally require one or more of the following factors for NW synthesis; high synthesis temperature, high vacuum environment, hazardous gas precursor and sophisticated instrumentation. To overcome these drawbacks, self-selective electroless etching based on localized electrochemical redox reactions has recently been proposed where, for $AgNO_3$:HF:Si system, SiNW arrays and silver dendrite coatings were obtained on the Si substrate surface [4,5].

Materials and methods

Randomly-oriented SiNWs were fabricated via the SLS process on gold-coated Si(100) substrates. Different stages of NW formation were achieved by selectively controlling the growth times and Au catalyst layer thicknesses. The growth chamber of the furnace was evacuated to 10^{-3}

Torr with cyclic nitrogen purging prior to growth to reduce the residual gasses present. It was then gradually heated to and maintained at 1000°C under constant purified nitrogen flow throughout the annealing process to minimize oxidation during growth. For the synthesis of vertically-oriented SiNW arrays, high-grade Si(001) substrates were cleaned and etched in an electrolyte bath containing aqueous solution of 0.04 M $AgNO_3$ and 5 M HF. The etching time was systematically varied between 15 - 120 minutes and the etching temperature ranged from room temperature to 50°C. The as-prepared samples were then etched in 6 M HNO_3 to remove the dense silver dendrite overgrowths to reveal arrays of well-aligned SiNWs underneath. Te-Si and Bi_2Te_3-Si core-shell structures were subsequently obtained by galvanic displacement of SiNWs in an acidic HF electrolyte containing $HTeO_2^+$ and $Bi^{3+}/HTeO_2^+$ ions respectively. This was done by immersing the SiNW arrays or free-standing SiNWs into 0.01 M of TeO_2 in 5 M HF or 0.01 M TeO_2 + 0.008M $Bi(NO_3)_3.5H_20$ in 5 M HF, maintained at different temperatures for different durations.

Results and discussion

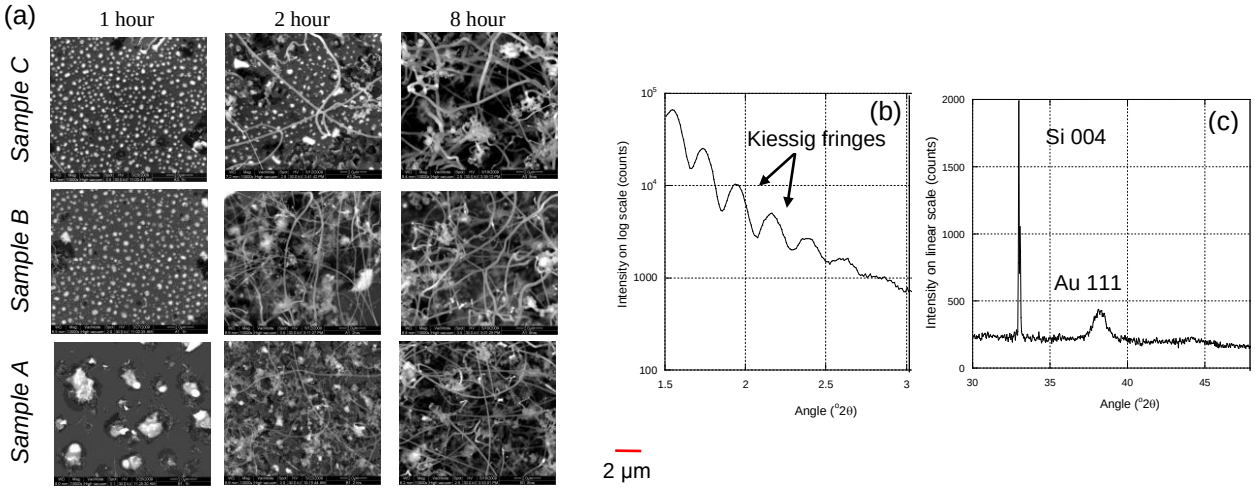

Fig. 1: (a) Series of top-view SEM images showing the evolution of NW morphology with growth duration and catalyst layer thickness. Catalyst layer thicknesses for A, B and C were 15 nm, 23 nm and 120 nm respectively and the growth temperature for all the samples was fixed at 1000°C. (b) Low-angle X-ray diffractogram of a Au-coated Si substrate (for sample B) showing the occurrence of Kiessig fringes and (c) high-angle X-ray diffractogram from the same sample.

Fig. 1 is a series of top-view SEM images taken at same magnification for three representative samples (A, B and C) showing different stages of NW formation via the SLS process under different growth durations and Au catalyst layer thicknesses. The exact thickness of the Au catalyst layer for each sample was determined from the angular spacings of the Kiessig fringes in low-angle X-ray diffractograms (Fig. 1b). High-angle X- ray diffractogram from the sample in Fig. 1c shows only the presence of Au and Si peaks, indicating the purity of the gold catalyst layer used. Generally, the NWs showed a variation in external morphology as a function of growth duration and gold catalyst layer thickness as observed in Fig. 1.

Typical diameters of the Au-Si eutectic catalyst droplets after 1 hour of annealing was approximately 150 to 550 nm as seen in Fig. 1 for A and C. Samples that have been annealed for 2 to 8 hours showed dense growth of SiNWs with smooth external morphology and large aspect ratios. Most of the wires were straight with uniform thickness along their lengths except for some worm-like structures. Although the exact lengths of the NWs were difficult to measure, their diameters ranged from ~ 50 to 350 nm and their lengths generally extended over several µm up to tens of µm. Typical high-angle X-ray diffractograms recorded from the samples revealed that the NWs were, in general, crystalline as shown in Fig. 2a. Figure 2b and c are the TEM bright-field

images of a worm-like and a straight SiNWs respectively. TEM selected-area diffraction patterns (SADPs) recorded from the samples (insets) show that the worm-like structure was amorphous while the straight NW was crystalline.

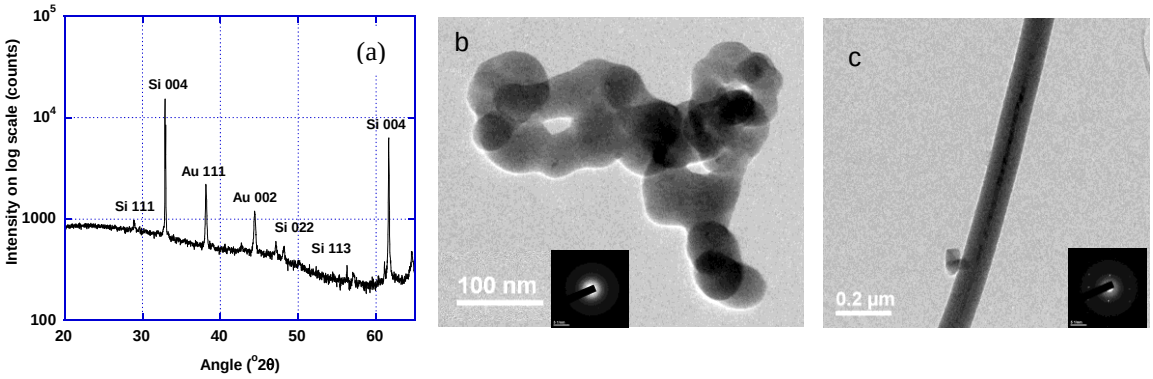

Fig. 2: (a) High-angle X-ray diffractogram of a NW sample after 6 hours of annealing. TEM bright-field images of (b) a worm-like amorphous and (c) a straight crystalline SiNWs.

SiNWs obtained via the electroless etching process were initially covered with thick films of metallic silver particles and tree-like silver dendrite overgrowths (Figure 3a and b). Dendrite formation was more prominent and denser with increasing etching time as may be inferred by comparing the Ag/Si peak intensity ratios for the EDX traces in Fig. 3 (a) and (b).

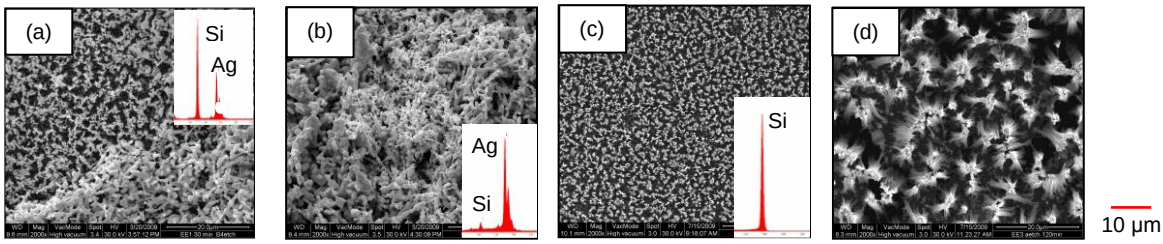

Fig. 3: Top-view SEM images. (a) and (b) Typical morphologies of the silver dendrite overgrowths for etching durations of 30 and 120 min. respectively. (c) and (d) The same samples after removal of silver dendrite overgrowths, revealing dense SiNW arrays underneath.

Upon removal of the silver dendrite overgrowths using HNO_3 aqueous solution, large-area of well-aligned SiNW arrays were seen self-assembled on the Si substrates (Fig. 3c and d). The SiNW arrays were of high chemical purity as indicated by the EDX spectra in the absence of Ag dendrites (Fig. 3c). Free ends of the NWs tend to bundle into clusters of increasing sizes as the NWs grew in length with longer etching durations. Generally, the length of the NWs varied as a function of etching time and electrolyte temperature. Fig. 4a and b show, representatively, the cross-sectional SEM images from a series of SiNW arrays (etched at 40°C) for different etching durations. Fig. 4c and d are the representative cross-sectional SEM images from a series of SiNW arrays obtained at a fixed etching duration of 120 min but at different etching temperatures. SEM observations reveal that the length of the SiNW arrays increased steadily from ~ 10 to 40 μm when the etching time was increased from 30 to 120 minutes and from ~ 20 to 40 μm when the etching temperature was increased from room-temperature to 50°C.

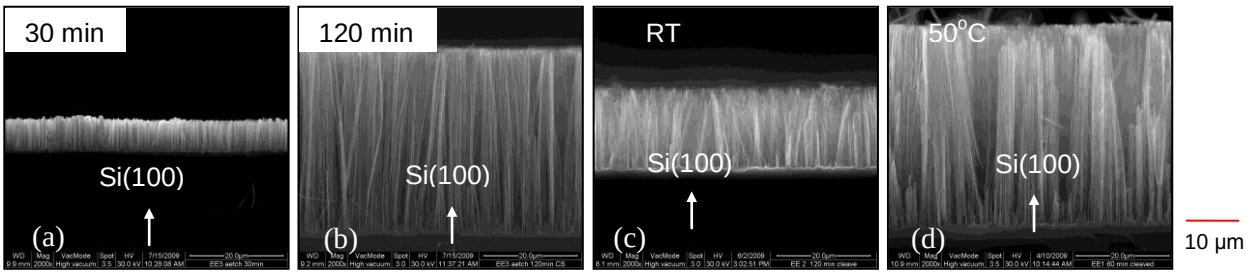

Fig. 4: Representative cross-sectional SEM images of the SiNW arrays. (a) and (b) NWs synthesized at 40°C showing variation in length as a function of etching time. (c) and (d) NWs etched for 120 min showing variation in length as a function of etching temperature.

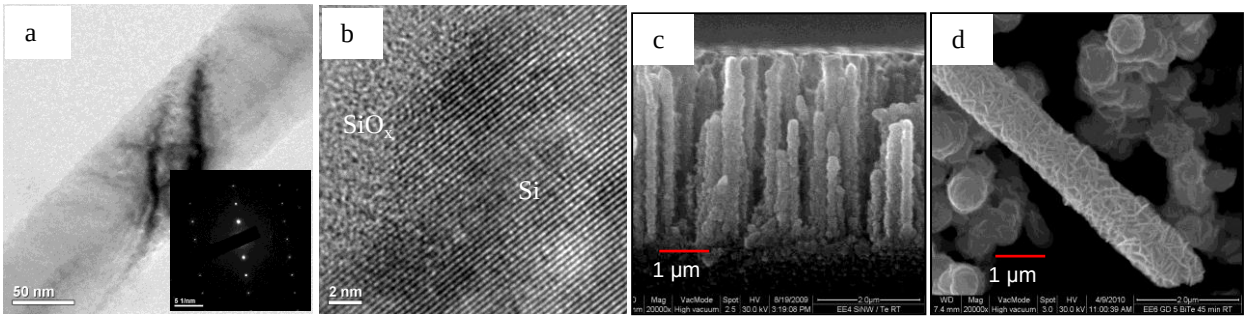

Fig. 5: (a) TEM bright-field image of a SiNW. Inset: The corresponding Si single-crystal diffraction pattern recorded from the NW. (b) HRTEM image of a section of the NW in (a) showing single-crystalline Si core and amorphous SiO_x sheath. (c) and (d) SEM images of a Te-Si and a Bi_2Te_3-Si core-shell structures.

Fig. 5a is the TEM bright-field image of a single SiNW. HRTEM image of the NW in Fig. 5b shows a single-crystalline silicon core surrounded by an amorphous sheath which is most likely to be the native SiO_x formed due to extended air exposure after NW synthesis. The corresponding Si single-crystal diffraction pattern from the core is shown in the inset in Fig. 5a.

Te-Si and Bi_2Te_3-Si core-shell structures were subsequently produced via post-growth modification of the SiNWs. This was done by galvanically displacing SiNWs from Te or Bi_2Te_3 in an acidic HF electrolyte containing $HTeO_2^+$ and $Bi^{3+}/HTeO_2^+$ions respectively. This was an electrochemical process brought about by the difference in redox potentials between the materials. SiNW arrays or free-standing SiNWs were immersed into 0.01 M of TeO_2 in 5 M HF solution or 0.01 M TeO_2 + 0.008M $Bi(NO_3)_3.5H_20$, in 5 M HF maintained at different temperatures and for different durations. Representative SEM image in Fig. 5c shows an array of Te-Si core-shell structures on Si substrate obtained via the galvanic displacement process for 30 minutes at room-temperature. Fig. 5d shows a typical Bi_2Te_3-Si core-shell structure obtained via the same process for 45 minutes at room temperature. The core-shell structures in both cases exhibit roughened surface morphologies. TEM images in Fig. 6 show the Te-Si core-shell structures exhibiting thorn-like surface morphology. The selected area diffraction pattern (SADP) indicates the polycrystalline nature of the roughened Te outer layer.

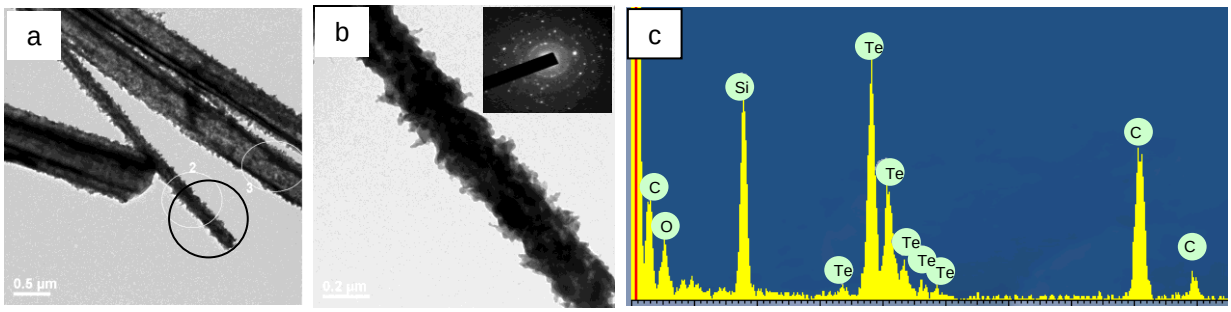

Fig. 6: (a) TEM bright-field image of a cluster of Te-Si core-shell structures, (b) Magnified image from the circled region in (a) and (c) EDX spectrum from the Te-Si core-shell structure.

Conclusions

A mixture of freely-oriented, crystalline and amorphous SiNWs was successfully synthesized via the SLS process at 1000°C using Si-supported gold mono-dispersed catalyst. Vertically well-aligned single-crystalline SiNW arrays were also produced on Si (100) substrates via self-selective electroless etcching where selective lengths of the SiNWs were tunable by controlling the growth parameters. We have also demonstrated that Te-Si and Bi_2Te_3-Si core-shell structures with roughened surface morphologies could subsequently be obtained via post-growth galvanic displacement of SiNWs from aqueous TeO_2 or $TeO_2/Bi(NO_3)_3$ in HF.

Acknowledgements

The authors acknowledge B. T. Goh, S. K. Chong and S. Abdul Rahman (University of Malaya) for the SLS growth of SiNWs and Z. Selamat (Malaysian Nuclear Agency) for SEM work. This work was supported by the Malaysian Government under Grant # 03-03-01-SF0031.

References

[1] L. Schubert, P. Werner, N. D. Zakharov, G. Gerth, F. M. Kolb, L. Long, U. Gösel, T. Y. Tan, *Appl. Phys. Lett.*, **84** (24), p 4968..
[2] R. S. Wagner and W. C. Ellis, *Appl. Phys. Lett*. **4** (1964), p 89.
[3] J. B. Chang, J. Z. Liu, P. X. Yan, L. F. Bai, Z. J. Yan, X. M. Yuan and Q. Yang, *Mater. Lett*. **60** (2006), p 2125.
[4] K. Q. Peng, Y. J. Yan, S. P. Gao and J. Zhu, *Adv. Mater*. **14** (16) (2002), p 1164.
[5] T. Qiu, X. L. Wu, G. G. Siu and P. K. Chu, *J. of Electronic Mater*. **35** (10) (2006), p 1879.

Nanomaterials
10.4028/www.scientific.net/AMR.364

Large-Area Synthesis and Microstructural Investigations of Silicon Nanowires and Te/Bi₂Te₃-Si Core-Shell Structures
10.4028/www.scientific.net/AMR.364.243

DOI References
[2] R. S. Wagner and W. C. Ellis, Appl. Phys. Lett. 4 (1964), p.89.
doi:10.1016/S0020-7403(64)80016-3

[3] J. B. Chang, J. Z. Liu, P. X. Yan, L. F. Bai, Z. J. Yan, X. M. Yuan and Q. Yang, Mater. Lett. 60 (2006), p.2125.
doi:10.1016/j.matlet.2005.12.085

[4] K. Q. Peng, Y. J. Yan, S. P. Gao and J. Zhu, Adv. Mater. 14 (16) (2002), p.1164.
doi:10.1002/1521-4095(20020816)14:16<1164::AID-ADMA1164>3.0.CO;2-E